Response of Plant-Insect Associations to Paleocene-Eocene Warming

Peter Wilf[1]* and Conrad C. Labandeira[1,2]

The diversity of modern herbivorous insects and their pressure on plant hosts generally increase with decreasing latitude. These observations imply that the diversity and intensity of herbivory should increase with rising temperatures at constant latitude. Insect damage on fossil leaves found in southwestern Wyoming, from the late Paleocene–early Eocene global warming interval, demonstrates this prediction. Early Eocene plants had more types of insect damage per host species and higher attack frequencies than late Paleocene plants. Herbivory was most elevated on the most abundant group, the birch family (Betulaceae). Change in the composition of the herbivore fauna during the Paleocene-Eocene interval is also indicated.

Terrestrial plants and insects today make up most of Earth's biodiversity (*1*), and almost half of insect species are herbivores (*2*). Consequently, understanding how plant-insect associations respond to warming events is a vital component of global change studies (*3*). The fossil record offers a unique opportunity to examine plant-insect response to climate change over long time intervals through analysis of insect damage on fossil plants (*4*, *5*).

In modern insect faunas, decreasing latitude is associated with increased diversity of insect herbivores per host plant and greater herbivore pressure; the latter is expressed as higher attack frequency (*6*, *7*). For this study, we used insect damage on fossil plants to test for these trends at constant latitude, in the context of the global warming interval that began in the late Paleocene and reached maximum Cenozoic temperatures by the middle early Eocene, about 53 million years ago (*8*). We also examined whether the diversity of herbivory and increase in attack rates was highest on the most abundant hosts and addressed whether a compositional change in the Paleocene-Eocene herbivore fauna occurred.

The Great Divide, Green River, and Washakie basins of southwestern Wyoming, U.S.A. (Fig. 1), bear diverse and abundant floral assemblages containing well-preserved insect damage (Fig. 2 and Table 1) (*9*). We compared two floral samples from this region, from the latest Paleocene and middle early Eocene (*10*). Both samples were originally deposited in fine-grained sediments on humid, swampy floodplains (*9*), which allowed us to use an isotaphonomic (*11*) approach that helps to factor out biases such as depositional regime, paleotopography, and past moisture levels. Previous analysis of these samples (*9*, *12*) showed that, from the latest Paleocene to the middle early Eocene, (i) mean annual temperatures rose from an estimated 14.4° ± 2.5°C to 21.3° ± 2.2°C, (ii) plant species turnover exceeded 80%, (iii) all dominant plant species were replaced, and (iv) plant diversity increased significantly.

We identified 41 types of insect damage (Table 1 and Fig. 2) on 39 Paleocene and 49 Eocene species of terrestrial flowering plants at 49 Paleocene and 31 Eocene localities (Fig. 1) (*9*, *10*, *13*). A database was constructed in which the presence or absence of each damage type was scored for each species in each sample (Table 1). We also quantitatively took field censuses of the four plant localities with highest diversity and best preservation (two Paleocene and two Eocene) for insect damage on dicot leaves (*14*).

Census data were analyzed for all leaves and separately for Betulaceae and all non-betulaceous taxa. A single species of Betulaceae was a dominant component of the vegetation in both the Paleocene (*Corylites* sp.) and

[1]Department of Paleobiology, National Museum of Natural History, Smithsonian Institution, Washington, DC 20560–0121, USA. [2]Department of Entomology, University of Maryland, College Park, MD 20742–4454, USA.

*To whom correspondence should be addressed (after August 1999) at the Museum of Paleontology, University of Michigan, Ann Arbor, MI 48109–1079, USA. E-mail: pwilf@umich.edu

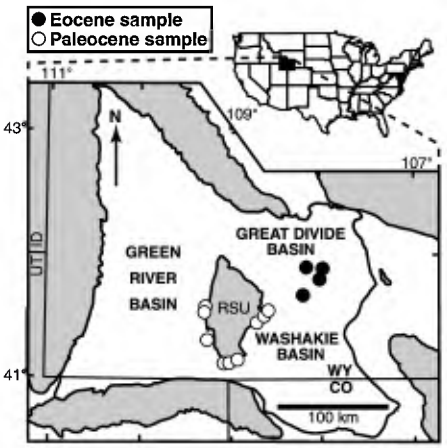

Fig. 1. Sampling areas. The most northeastern circle for each set includes the localities for insect damage censusing (Figs. 3 and 4). Gray areas are uplifts. RSU, Rock Springs Uplift. Redrawn after (*9*).

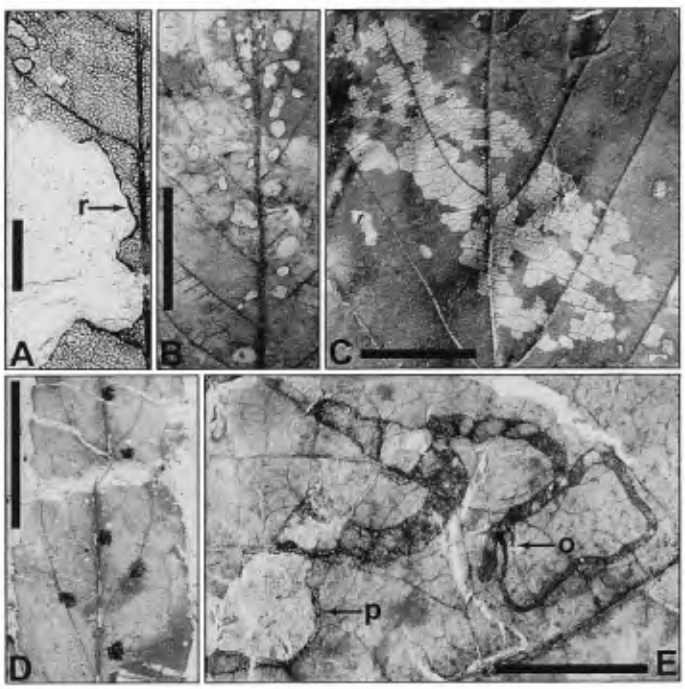

Fig. 2. Examples of Paleocene-Eocene insect damage. Panels (A) and (C) are Paleocene and (B), (D), and (E) are Eocene. All scale bars equal 1 cm. (**A**) Margin feeding to primary vein on *Persites argutus* Hickey (Lauraceae), USNM 498036, USNM locality (loc.) 41292. Note thick reaction tissue (r). (**B**) Polymorphic, elliptical hole feeding on *Alnus* sp. (Betulaceae), USNM 498177, USNM loc. 41339. Note reaction tissue bordering holes. (**C**) Broad, rectangular skeletonization of *Corylites* sp. (Betulaceae), USNM 498176, USNM loc. 41270. Note fine detail of exposed venation. (**D**) Galls on primary and secondary veins of *Stillingia casca* Hickey (Euphorbiaceae), USNM 498175, USNM loc. 41341. (**E**) Serpentine mine (type E) on new dicot sp. RR37, USNM 498091, USNM loc. 41353. The mine crosses tertiary and higher order veins. The oviposition site (o) and the site of the pupation chamber (p) are both preserved.

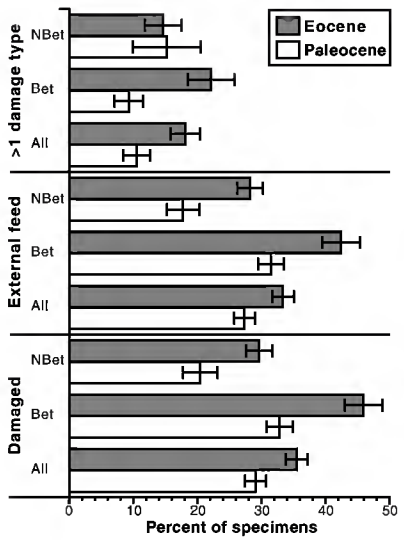

Fig. 3. Damage census data. From bottom to top: leaves with any insect damage, leaves externally fed, and the percentage of damaged leaves bearing more than one damage type (Table 1). These categories are each analyzed separately for all leaves (All), Betulaceae only (Bet), and non-Betulaceae only (NBet). Error bars are one standard deviation of binomial sampling error (*27*). Sample sizes for Paleocene and Eocene, respectively: All (749, 791); Bet (524, 285); and NBet (225, 506). Total leaf area examined in censuses, derived from Webb leaf-area categories (*28*): 2.26 m^2 (Paleocene) and 2.12 m^2 (Eocene). Paleocene = USNM locs. 41270 and 41300 combined; Eocene = USNM locs. 41342 and 41352 combined.

Table 1. Insect damage types. The presence (+) or absence (−) of each type in the Paleocene (Pal) and Eocene (Eoc) samples is indicated and their relative degree of specialization (Spec): 1 = most generalized, 3 = most specialized. Terminology modified from (*26*). Genus names or morphotype numbers of host plant species are listed for the most specialized damage types and those that exhibit turnover (*9*).

Damage type	Pal	Eoc	Spec
External feeding			
Constant width, elongate, branching	+	+	2
Strip-feeding between secondary veins (*Zingiberopsis*)	−	+	3
Window feeding, generalized	+	+	1
Hole feeding			
Generalized, unpatterned	+	+	1
Bud feeding (*Alnus*, *Hovenia*, *Schoepfia*)	−	+	2
Curvilinear	+	+	2
Elliptical	+	+	1
Elongated slot	+	+	2
Large, ovoidal or circular	+	+	1
Large, polylobate	+	+	1
Exceptionally thick necrotic tissue	+	+	1
Polymorphic, generally elliptical	+	+	2
Ring (aff. *Ocotea*)	+	−	1
Small, ovoidal or circular	+	+	1
Small, polylobate	+	+	1
Margin feeding			
Generalized, usually cuspate	+	+	1
Apex feeding	+	+	1
Free feeding (*Platycarya*, *Populus*)	−	+	2
To primary vein	+	+	1
Trenched (deeply incised)	+	+	2
Skeletonization			
General, reaction rim weak	+	+	1
General, reaction rim well developed	+	+	1
Broad, with rectangular pattern (*Corylites*)	+	−	2
Curvilinear (*Persites*)	+	−	2
Highest order venation removed (*Platycarya*)	−	+	2
Linear pattern (*Alnus*)	−	+	2

Damage type	Pal	Eoc	Spec
Skeletonization (cont.)			
Ovoidal, adjacent to midvein	+	+	2
Multiple, subparallel, curvilinear tracks (*Corylites*, new dicot sp. RR31)	+	+	3
Mining			
Blotch, central chamber (*Persites*, Magnoliales sp., aff. *Sloanea*)	+	+	3
Blotch, large (>2 cm diam.), no central chamber ("*Ampelopsis*")	+	−	3
Circular, with case (*Corylites*)	+	−	3
Serpentine A: long, undulatory; frass particulate (*Corylites*, *Alnus*, *Cinnamomophyllum*, new dicot sp. RR20)	+	+	3
Serpentine B: length medium, width rapidly increasing, margin irregular (*Corylites*)	+	−	3
Serpentine C: length short, frass trail solid ("*Dombeya*", cf. Magnoliales sp. RR12, *Alnus*)	−	+	3
Serpentine D: long, frass tightly sinusoidal, frass trail narrow (*Cinnamomophyllum*)	−	+	3
Serpentine E: length medium, margin irregular, oviposition site and terminus well defined (new dicot sp. RR37)	−	+	3
Galling			
On blade, other than major veins	+	+	2
On primary vein(s) only	+	+	2
On secondary veins only	+	+	2
Piercing and sucking			
Scale or puncture, circular depression (Magnoliaceae sp. FW07, palm leaf, new dicot sp. RR48)	+	+	3
Scale or puncture, elliptical depression (palm leaf)	+	−	3

the Eocene (*Alnus* sp.) (*15*). These two species fit the traditional model of "apparent" plants in that they were abundant, conspicuous hosts that formed significant ecological islands (*16*). Like all modern Betulaceae, whose leaves are heavily consumed by insects (*17*, *18*), *Corylites* and *Alnus* (alder) were thin-leaved and deciduous, adding to their presumed palatability (*7*, *19*). We hypothesized that these taxa were frequently consumed by a high diversity of herbivores.

The census data show that, overall, damage frequency is significantly higher in the Eocene sample, indicating elevated levels of herbivory (Fig. 3) (*20*). Betulaceous leaves were attacked significantly more often than nonbetulaceous leaves within both sampling levels, and their damage frequency (Fig. 3), multiple damage frequency (Fig. 3), and damage diversity (Figs. 4 and 5) increased markedly from the Paleocene to the Eocene (*21*). *Alnus* palatability was probably enhanced by elevated leaf nitrogen content resulting from an actinorhizal association with nitrogen-fixing symbionts, as in all modern *Alnus* (*18*, *22*).

Bootstrap curves derived from the census data (Fig. 4) show increased minimum and maximum damage diversity at a local scale during the Eocene. All of the Paleocene taxa except one (aff. *Ocotea*) have nearly identical bootstrap curves. Four Eocene species have bootstrapped values higher than all of the Paleocene taxa (*Alnus*, *Cinnamomophyllum*, "*Dombeya*", and *Populus*). Three other Eocene species have bootstrap values that are lower than the Paleocene mode represented by *Corylites* (*Allophylus*, Apocynaceae sp., and aff. *Sloanea*) but still higher than the Paleocene minimum (aff. *Ocotea*).

The diversity of insect damage per host species increases with the percentage of localities where a given host occurred because increased sampling raises the probability of discovering damage types (Fig. 5). However, when comparison is made at equal frequency of occurrence, greater herbivore diversity per host plant is again found in the Eocene than in the Paleocene. The Eocene slope in Fig. 5 is higher, even though 37% fewer localities are in the Eocene sample and less geologic time is represented (*10*). Also, the five largest positive residuals are all Eocene species. Finally, the single abundant monocot (Eocene *Zingiberopsis*) has a large effect. If dicots alone are considered, the Eocene slope increases another 15% (*23*).

A change in the composition of the herbivore fauna is indicated (Table 1). In all, 17% of damage types only occur in the Paleocene sample, whereas 20% of damage types are only found in the Eocene sample. Each of the generalized damage types (scores of 1 in Table 1) may have been caused by several groups of distantly related insects. If only the 27 specialized damage types are counted (scores of 2 or 3 in Table 1), Paleocene-only types are 22% and Eocene-only types 30% (*24*).

This study demonstrates that the effects of global warming on plant-insect interactions are detectable in the fossil record. Climate change also provides a largely unexplored context for related areas of inquiry, such as the histories of plant-pollinator relations and insect diversification.

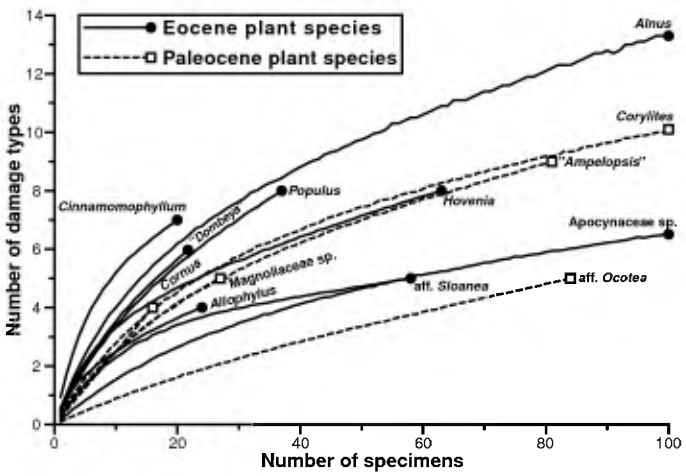

Fig. 4. Bootstrapped damage diversity, derived from the census data, for species with >15 specimens in total census counts. For each positive integer n along the horizontal axis up to the total number of specimens for a species (N), 5000 subsamples of n specimens were taken at random and the mean number of damage types calculated (vertical axis). The line graphs connect the N mean values for each species. Shown only to $n \leq 100$ for greater detail. Maximum $\sigma = 1.8$ (for *Alnus*, $n = 80$). Family or generic names only are shown; see (9) for complete nomenclature. "aff." = morphological affinity to indicated genus, a qualified identification.

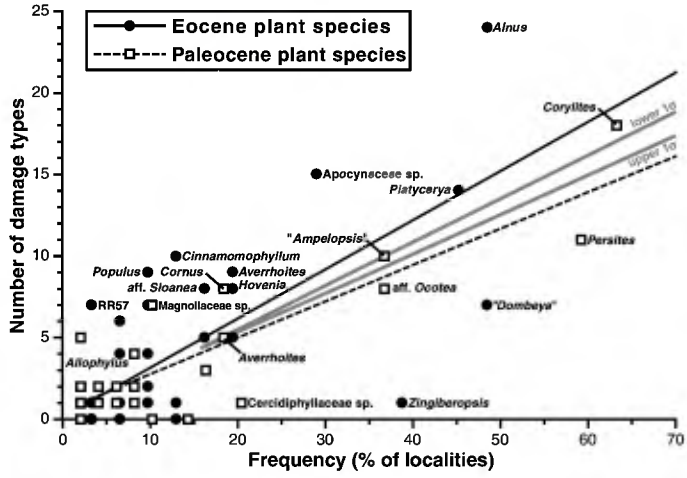

Fig. 5. Diversity of insect damage per plant host species (vertical axis), plotted against the percentage of localities (49 Paleocene, 31 Eocene) at which the species occurs. Each data point is one species; many data points overlap at the lower left; survivors are plotted twice. Gray lines show divergence of 1σ (68%) confidence intervals for the two regressions. Paleocene regression: $y = 22.3x + 0.545$, $r^2 = 0.775$, $P < 10^{-12}$ (r^2 is the coefficient of determination). Eocene regression: $y = 30.1x + 0.117$, $r^2 = 0.538$, $P < 10^{-8}$. Family or generic names are shown for plant species that are abundant, plot with large residuals, or appear in Fig. 4.

References and Notes

1. N. E. Stork, *Biol. J. Linn. Soc.* **35**, 321 (1988).
2. L. M. Schoonhoven, T. Jermy, J. J. A. van Loon, *Insect-Plant Biology* (Chapman & Hall, London, 1997).
3. E. D. Fajer, M. D. Bowers, F. A. Bazzaz, *Science* **243**, 1198 (1989); R. L. Lindroth, K. K. Kinney, C. L. Platz, *Ecology* **74**, 763 (1993); J. A. Arnone, J. G. Zaller, C. Ziegler, H. Zandt, C. Körner, *Oecologia* **104**, 72 (1995); R. A. Fleming, *Silva Fenn.* **30**, 281 (1996); C. S. Awmack, R. Harrington, S. R. Leather, *Global Change Biol.* **3**, 545 (1997); P. D. Coley, *Clim. Change* **39**, 455 (1998); S. J. Dury, J. G. Good, C. M. Perrins, A. Buse, T. Kaye, *Global Change Biol.* **4**, 55 (1998); J. B. Whittaker and N. P. Tribe, *J. Anim. Ecol.* **67**, 987 (1998).
4. C. C. Labandeira, D. L. Dilcher, D. R. Davis, D. L. Wagner, *Proc. Natl. Acad. Sci. U.S.A.* **91**, 12278 (1994); C. C. Labandeira, *Annu. Rev. Earth Planet. Sci.* **26**, 329 (1998).
5. A. L. Beck and C. C. Labandeira, *Palaeogeogr. Palaeoclimatol. Palaeoecol.* **142**, 139 (1998).
6. T. L. Erwin, *Coleopt. Bull.* **36**, 74 (1982); P. D. Coley and T. M. Aide, in *Plant Animal Interactions: Evolutionary Ecology in Tropical and Temperate Regions*, P. W. Price, T. M. Lewinsohn, G. W. Fernandes, B. B. Benson, Eds. (Wiley, New York, 1991), pp. 25–49; P. D. Coley and J. A. Barone, *Annu. Rev. Ecol. Syst.* **27**, 305 (1996); M. G. Wright and M. J. Samways, *Oecologia* **115**, 427 (1998).
7. Y. Basset, *Acta Oecol.* **15**, 181 (1994).
8. M.-P. Aubry, S. G. Lucas, W. A. Berggren, Eds., *Late Paleocene-Early Eocene Climatic Events in the Marine and Terrestrial Records* (Columbia Univ. Press, New York, 1998). Mean annual temperatures increased 7° to 9°C in the Rocky Mountain region from the latest Paleocene to the middle early Eocene (9, *25*), and sea surface temperatures in southern high latitudes rose from between 10°–12° to 14°–16°C, the latter 13° to 15°C warmer than today [J. C. Zachos, L. D. Stott, K. C. Lohmann, *Paleoceanography* **9**, 353 (1994)]. A significant atmospheric increase in the partial pressure of CO_2 has been postulated as a cause of Paleocene-Eocene warming [D. K. Rea, J. C. Zachos, R. M. Owen, P. D. Gingerich, *Palaeogeogr. Palaeoclimatol. Palaeoecol.* **79**, 117 (1990)], but this hypothesis is not yet supported by proxy and model data [E. Thomas, in *Late Paleocene–Early Eocene Climatic and Biotic Events in the Marine and Terrestrial Records*, M.-P. Aubry, S. G. Lucas, W. A. Berggren, Eds. (Columbia Univ. Press, New York, 1998), pp. 214–235].
9. P. Wilf, *Geol. Soc. Am. Bull.*, in press.
10. The late Paleocene sample is sample 2 of (9), a lumped Clarkforkian assemblage. The Eocene sample, from the Cenozoic thermal maximum, is the middle Wasatchian Sourdough flora, Great Divide Basin, sample 5 of (9). The Paleocene sample is time-averaged over ~0.5 million years, during which some temperature increase occurred (9, *12*, *25*), whereas the more diverse Eocene sample is not significantly time-averaged and is derived from fewer localities. A total leaf count was not made because not all identifiable specimens were collected from every locality. An unbiased measure is that 7511 leaves have been identified from the 15 localities that were censused on the outcrop (9); the total number of leaves examined from all 80 localities was far greater. Although floras from intervening stratigraphic intervals are known (9), the two samples used here are among the best preserved and are derived from many more localities. Deciduous taxa were more abundant than evergreens in both samples, although evergreens were more diverse in the Eocene sample (9). "Species" is used here to indicate both described species and undescribed forms considered as operational species in (9). Voucher collections, from the 1994 to 1996 and 1998 field seasons, are housed at the U.S. National Museum of Natural History (USNM), with supplementary material at the Denver Museum of Natural History and the Florida Museum of Natural History (9).
11. A. K. Behrensmeyer and R. W. Hook, in *Terrestrial Ecosystems Through Time*, A. K. Behrensmeyer *et al.*, Eds. (Univ. of Chicago Press, Chicago, IL, 1992), pp. 15–136.
12. P. Wilf, K. C. Beard, K. S. Davies-Vollum, J. W. Norejko, *Palaios* **13**, 514 (1998).
13. A damage type (Table 1) was assigned if a distinctive insect feeding mode, or ecotype, was represented. No damage was found on conifers, cycads, or aquatic angiosperms, and damage on ferns was rare.
14. The primary goal of initial collecting (1994 to 1996 field seasons) was to reconstruct floral diversity and leaf morphology, with some resulting collection bias against common species and consequently against their insect damage. The field censusing of insect damage (in 1998) allowed unbiased sampling of herbivory on all species to complement that known from collections and also permitted the observed damage frequencies to be related as directly as possible to the relative abundances of host plants in the source forests [R. J. Burnham, S. L. Wing, G. G. Parker, *Paleobiology* **18**, 30 (1992)].
15. The *Corylites* sp., from the Paleocene sample only, was described as the presumed foliage of *Palaeocarpinus aspinosa* Manchester and Chen [S. R. Manchester and Z. Chen, *Int. J. Plant Sci.* **157**, 644 (1996)]. The *Alnus* sp., undescribed, is known from leaves, female cones, and staminate inflorescences in early Eocene deposits of southern and northern Wyoming (9, *25*). These taxa occurred at the largest number of localities (Fig. 5) and also were most frequently the dominant species at individual localities (9).
16. D. H. Janzen, *Am. Nat.* **102**, 592 (1968); P. A. Opler, *Am. Sci.* **62**, 67 (1974); P. P. Feeny, in *Biochemical Interaction Between Plants and Insects*, J. Wallace and R. L. Mansell, Eds. (Plenum, New York, 1976), pp. 1–40.
17. J. Reichholf, *Waldhygiene* **10**, 247 (1974); J. M. Cobos-Suarez, *Bol. Sanid. Veg.* **14**, 1 (1988); B. Gharadjedaghi, *Anz. Schaedlingskd. Pflanz. Umweltschutz* **70**, 145 (1997); B. Gharadjedaghi, *Forstwiss. Centralbl.* **116**, 158 (1997); J. Oleksyn *et al.*, *New Phytol.* **140**, 239 (1998).
18. O. Q. Hendrickson, W. H. Fogal, D. Burgess, *Can. J. Bot.* **69**, 1919 (1991).
19. P. D. Coley, *Oecologia* **74**, 531 (1988).
20. Damage frequency in fossil floras has been significantly lower than modern values in several studies (*5*), as we find here. Although insect damage may well have increased through time, it is likely that several factors would make damage appear less prevalent in fossil assemblages, including taphonomic bias against damaged leaves, the rarity of complete fossil leaves, the inability to observe completely consumed leaves, and the low probability of preservation for minute damage types, such as piercing and sucking. We consider good preservation of leaves (highest order venation visible on the majority of specimens, more than half of the original leaf usually present) and a fine-grained matrix, as in this study, to be prerequisites for censusing of insect damage. Insect damage by its nature reduces the preservability of leaves by

creating tear points, although this bias needs to be quantified in actualistic studies.
21. *Corylites* and *Alnus* fit well with the resource availability hypothesis [P. D. Coley, J. P. Bryant, F. S. Chapin III, *Science* **230**, 895 (1985)] in which high herbivory rates are correlated with short leaf lifespan (*Corylites* and *Alnus* were deciduous), high growth rates and relatively early successional status (*Corylites* and *Alnus* had tiny, wind- or water-dispersed fruits and colonized disturbed environments on floodplains), and low concentrations of defensive compounds (implied).
22. G. Bond, in *Symbiotic Nitrogen Fixation in Plants*, P. S. Nutman, Ed. (Cambridge Univ. Press, Cambridge, 1976), pp. 443–474; C. P. Onuf, J. M. Teal, I. Valiela, *Ecology* **58**, 514 (1977); W. J. Mattson Jr., *Annu. Rev. Ecol. Syst.* **11**, 119 (1980); R. E. Ricklefs and K. K. Matthew, *Can. J. Bot.* **60**, 2037 (1982); J. J. Furlow, in *Magnoliophyta: Magnoliidae and Hamamelidae*, vol. 3 of *Flora of North America*, Flora of North America Editorial Committee, Ed. (Oxford Univ. Press, New York, 1997), pp. 507–538. Phylogenetic analysis of DNA sequences from the *rbcL* gene places all actinorhizal plants within a single clade, indicating that actinorhizal association is ancient [D. E. Soltis *et al.*, *Proc. Natl. Acad. Sci. U.S.A.* **92**, 2647 (1995)].
23. Insect damage on the single dicot species that was abundant in both samples (*Averrhoites affinis*) increased from five types in the Paleocene to nine in the Eocene (Fig. 5).
24. Although the most specialized damage types are rare, sampling was intensive (*10*, *14*), which supports our view that the inferred turnover of herbivores is not a sampling artifact. The percentages listed should be regarded as minima given the difficulty of evaluating the more generalized feeding groups.
25. S. L. Wing, H. Bao, P. L. Koch, in *Warm Climates in Earth History*, B. T. Huber, K. MacLeod, S. L. Wing, Eds. (Cambridge Univ. Press, Cambridge, 1999), pp. 197–237.
26. R. N. Coulson and J. A. Witter, *Forest Entomology: Ecology and Management* (Wiley, New York, 1984).
27. P. Wilf, *Paleobiology* **23**, 373 (1997).
28. L. J. Webb, *J. Ecol.* **47**, 551 (1959). The logarithmic mean area was used for each Webb category to estimate total leaf area [P. Wilf, S. L. Wing, D. R. Greenwood, C. L. Greenwood, *Geology* **26**, 203 (1998)].
29. We thank A. Ash, R. Schrott, K. Werth, and others for field and laboratory assistance, Western Wyoming Community College for logistical support, and W. DiMichele, P. Dodson, R. Horwitt, B. Huber, S. Wing, and two anonymous reviewers for helpful comments on the manuscript. P.W. was supported by Smithsonian Institution predoctoral and postdoctoral fellowships, the Smithsonian's Evolution of Terrestrial Ecosystems Program (ETE), a University of Pennsylvania Dissertation Fellowship, the Geological Society of America, Sigma Xi, and the Paleontological Society. C.C.L. was supported by the Walcott Fund of the National Museum of Natural History. This is ETE contribution number 68.

19 March 1999; accepted 5 May 1999

On the Weakening Relationship Between the Indian Monsoon and ENSO

K. Krishna Kumar,[1]*† Balaji Rajagopalan,[2] Mark A. Cane[2]

Analysis of the 140-year historical record suggests that the inverse relationship between the El Niño–Southern Oscillation (ENSO) and the Indian summer monsoon (weak monsoon arising from warm ENSO event) has broken down in recent decades. Two possible reasons emerge from the analyses. A southeastward shift in the Walker circulation anomalies associated with ENSO events may lead to a reduced subsidence over the Indian region, thus favoring normal monsoon conditions. Additionally, increased surface temperatures over Eurasia in winter and spring, which are a part of the midlatitude continental warming trend, may favor the enhanced land-ocean thermal gradient conducive to a strong monsoon. These observations raise the possibility that the Eurasian warming in recent decades helps to sustain the monsoon rainfall at a normal level despite strong ENSO events.

Most parts of India receive a major proportion of their annual rainfall during the summer (June to September) monsoon season. Extreme departures from normal seasonal rainfall, such as large-scale droughts and floods, seriously affect agricultural output and regional economies. By the early 1900s, investigators had identified the two large-scale forcings still thought to be most important for predicting monsoon anomalies: Himalayan/Eurasian snow extent (*1*) and the ENSO cycle (*2*). The former is generally believed to provide an indication of the pre-monsoon thermal condition over the Asian land mass. Warmer conditions are thought to aid the buildup of a strong land-sea thermal gradient during the summer (*3, 4*). ENSO, the largest known climatic forcing of interannual monsoon variability, acts through the east-west displacement of large-scale heat sources in the tropics (*5*). Numerous studies (*6*) have shown a significant simultaneous association between the monsoon rainfall over India and ENSO indices. However, secular variations in the relationships between monsoon rainfall and its predictors have also been noted (*7*). These variations have been found to be linked to changes in ENSO characteristics such as amplitude and period (*8*).

Almost all the statistical seasonal prediction schemes of monsoon rainfall rely heavily on the change in magnitude in various ENSO indices (*8, 9*) from winter [December to February (DJF)] to spring [March to May (MAM)]. Numerical general circulation models (GCMs) are also used for seasonal rainfall prediction. The monsoon simulated in these GCMs is more sensitive to the sea surface temperatures (SSTs) specified in the Pacific (*10*) than to other external boundary forcings. Hence, the success of seasonal forecasts of monsoon rainfall depends on the stationarity of the monsoon-ENSO relationship.

We used data on Indian monsoon rainfall, SST, velocity potential fields, and global surface temperatures (*11*) to examine the simultaneous relationship between the monsoon and ENSO during the last 142 years, and to explore possible roles for other climatic forcings.

Low-frequency variations in the monsoon rainfall and a widely used measure of ENSO, the NINO3 index (*11*), show a clear resemblance until the late 1970s (Fig. 1A), but diverge thereafter. This change reflects the recent modest increase in the monsoon rainfall despite an increase in the magnitude and frequency of ENSO warm events. Sliding correlations on a 21-year moving window between monsoon rainfall and the NINO3 index are strong during the entire data period with the exception of the recent two to three decades (Fig. 1B), not withstanding the considerable impact of the 1982 and 1987–88 ENSO events on the monsoon. The drop in correlations in the recent decades is found to be significant on the basis of bootstrap confidence limits (*12*). The loss of monsoon-ENSO correlation is not particular to NINO3, but appears with any ENSO index. Correlation patterns of monsoon rainfall with SSTs in the Pacific show a coherent region of strong correlations in the central and eastern equatorial Pacific before 1980 and no region with statistically significant correlations thereafter.

The conventional description of the ENSO-induced teleconnection response in the monsoon is through the large-scale east-west shifts in the tropical Walker circulation. During an El Niño event, the tropical convection and the associated rising limb of the Walker circulation normally located in the western Pacific shift toward the anomalously

[1]International Research Institute (IRI) for Climate Prediction, Lamont-Doherty Earth Observatory (LDEO) of Columbia University, Post Office Box 1000, Route 9W, Palisades, NY 10964–8000, USA. [2]LDEO of Columbia University, Post Office Box 1000, Route 9W, Palisades, NY 10964–8000, USA.

*Permanent address: Indian Institute of Tropical Meteorology, Dr. Homi Bhabha Road, Pashan, Pune 411008, India.

†To whom correspondence should be addressed. E-mail: krishna@iri.ldeo.columbia.edu